Bull. Mater. Sci., Vol. 37, No. 6, October 2014, pp. 1375–1382. © Indian Academy of Sciences.

Preparation and characterization of Fe–V/TiO_2–SiO_2 nanocatalyst modified by zinc

MOSTAFA FEYZI, HAMID REZA RAFIEE* and FATANEH JAFARI

Department of Physical Chemistry, Faculty of Chemistry, Razi University, Kermanshah 67149, Iran

MS received 22 June 2013; revised 3 September 2013

Abstract. The Fe–V/TiO_2–SiO_2 nanocatalyst promoted with zinc is prepared by combination of sol–gel and wetness impregnation methods. The effects of different weight percentages of iron, vanadium and zinc, titania to silica mole ratio, synthesis temperature and heating rate of calcination on the structure and morphology of nanocatalyst are investigated. Results showed that the modified nanocatalyst containing 40 wt% of Fe, 12 wt% of V and 2 wt% of zinc (all on weight percent) supported on TiO_2–SiO_2 with synthesis temperature of 45 °C has highest surface area, pore volume and pore diameter. Characterizations of catalysts were carried out using X-ray diffraction (XRD), Fourier transform infrared (FT-IR) spectrometry, scanning electron microscopy (SEM), vibrating sample magnetometry (VSM) and N_2 physisorption measurements. It was found that the nanocatalyst has a particle size about 56 nm and its saturation magnetization factor is equal to 10·173 emu/g. The catalyst can easily be separated from medium by a magnet.

Keywords. Nanocatalyst; TiO_2–SiO_2; sol–gel; impregnation; magnetization.

1. Introduction

Magnetic nanosized transition metal oxides are propounded as inspiring catalysts for various reactions, particularly oxidation of organic compounds (Tsang *et al* 2004). The kind of support has an important effect on the catalytic properties and by the use of an allocated support, the activity and selectivity of the catalyst can be ameliorated (Hu and Waches 1995). By using a combination of titania and silica as a support, their intrinsic characteristics can be detected. Therefore the combined TiO_2–SiO_2 mixed oxide shows a novel category of materials that is in favour as a support (Samantaray and Parida 2001; Rana *et al* 2003; Kobayashi *et al* 2005). Such advanced titania–silica materials not only take benefit of both TiO_2 (an *n*-type semiconductor and an active catalytic support) and SiO_2 (high thermal stability and excellent mechanical strength), but this support also has the ability of dispersion of active metals such as V and Zn, creation of new catalytic active sites due to the interaction of TiO_2 with SiO_2, developed their applications (Gao and Wachs 1999). Vanadia-based catalysts play a major role in the petrochemical industry, to utilize for the synthesis of intermediates, pollution abatement and transformation of cheap feed stocks into added value products (Goehre and Friedrichsen 1969; Van Hengstum *et al* 1983). These catalysts are used in various formulations, among which vanadia supported on titania (anatase phase) is recognized to be an effective catalyst in partial oxidation of hydrocarbons. The major objection of titania as support is its low mechanical strength and ease of sintering. Moreover, at high temperatures, vanadia promotes the TiO_2 phase transition, from anatase to rutile (Vejux and Courtine 1978). This crystallographic rearrangement decreases the catalytic activity and selectivity of vanadia/titania toward partial oxidation products. To defeat such drawbacks, titania–silica composite supports, in the form of both mixed and layered oxides, are considered suitable materials for deposition of vanadia (Handy *et al* 1992; Dias *et al* 1997; Lakshmi *et al* 1997; Gutiérrez-Alejandre *et al* 1998; Gao *et al* 1999). Chemical promoters, such as K, Cu, Ru, Zn, etc. are often added into iron-based catalyst, to improve the attrition resistance of catalysts without sacrificing their activities and selectivities. (Arakawa and Bell 1983; Li *et al* 2002; Yang *et al* 2004; Zhang *et al* 2005, 2006). Further development of the catalytic system will require advanced materials that can selectively catalyze chemical reactions with high reactivity and be recycled through simple separation and regeneration processes. In the present study, we report the synthesis of Fe–V/TiO_2–SiO_2 nanocatalysts promoted with zinc which is prepared by the combination of sol–gel and wetness impregnation methods and characterized using X-ray diffraction (XRD), Fourier transform infrared (FT-IR) spectrometry, scanning electron microscopy (SEM), vibrating sample magnetometer (VSM) and N_2 physisorption measurements. The special characters of Fe–V/TiO_2–SiO_2 nanocatalyst promoted with zinc, are long half-life and

*Author for correspondence (rafieehr@yahoo.com)

high performance. Also, this catalyst can be separated by a magnet from the medium in any solvent.

2. Experimental

2.1 *Catalyst preparation*

All materials with analytical purity are purchased from Merck and used without further purification. The catalysts used in present study were prepared by a combination of sol–gel and wetness impregnation methods. The synthesis of Fe–V/TiO_2–SiO_2 promoted with zinc has 3 steps. At first, $Fe(NO_3)_3{\cdot}9H_2O$, tetraethyl orthosilicate (TEOS) and titanium isopropoxide (TIP) have been dissolved in ethanol then, were heated to 45 °C and stirred for 10 min. Later oxalic acid was added to the mixture under rigorous stirring. While the temperature kept at 45 °C, the homogeneous solutions, obtained almost after 90 min, have been left at room temperature and air atmosphere to jellify. The obtained gel was dried in the oven at 100 °C for 10 h to give a material denoted as the catalyst precursor. After drying and milling, precursor had been thermally treated (calcination) at 450 °C for 6 h to give the Fe/TiO_2–SiO_2 catalyst. In next steps, Fe/TiO_2–SiO_2 as a precursor was impregnated with aqueous solution of NH_4VO_3 and $Zn(NO_3)_2{\cdot}6H_2O$, respectively. At each step, new precursor has been dried in the drying oven at 100 °C for 10 h and has been thermally treated at 450 °C for 6 h, final catalyst is Fe–V/TiO_2–SiO_2 promoted with zinc (figure 1).

2.2 *Sample characterization*

2.2a *X-ray diffraction (XRD)*: The XRD patterns of the precursor and calcined samples were recorded on a Philips X'Pert (40 kV, 30 mA) X-ray diffractometer, using a CuKα radiation source (λ = 1·542 Å) and a nickel filter in the 2θ range of 4–90°.

2.2b *N_2-adsorption–desorption measurements*: The specific surface area (using BET method), total pore volume and the mean pore diameter were measured using a N_2 adsorption–desorption isotherm at liquid nitrogen temperature (–196 °C), using a NOVA 2200 instrument (Quantachrome, USA). Prior to measurements, all the samples were degassed at 110 °C in a N_2 flow for 3 h to remove the moisture and other adsorbates.

2.2c *Scanning electron microscopy (SEM)*: The morphologies of prepared samples and their precursors were observed by means of an S-360 Oxford Eng scanning electron microscope (USA).

2.2d *Fourier transform infrared (FT-IR) spectrometry*: FT-IR spectra were recorded with an ALPHA (Bruker, Germany) FT-IR spectrophotometer, equipped with a deuterium triglycine sulphate (DTGS) detector. Samples of 1–2 mg were mixed with 100 mg KBr and pressed into translucent disks at room temperature. All spectra were taken in the range 400–4000 cm^{-1} at a resolution of 4 cm^{-1}. The spectra of samples were presented by subtracting the background spectrum.

2.2e *Vibrating sample magnetometer (VSM)*: The magnetic measurement of optimal catalyst was carried out in a vibrating sample magnetometer (VSM, BHV-55, Riken, Japan) at room temperature.

3. Results and discussion

3.1 *Effect of synthesis temperature*

Synthesis temperature is an effective factor on porosity and surface area of nanocatalyst. To indicate this and

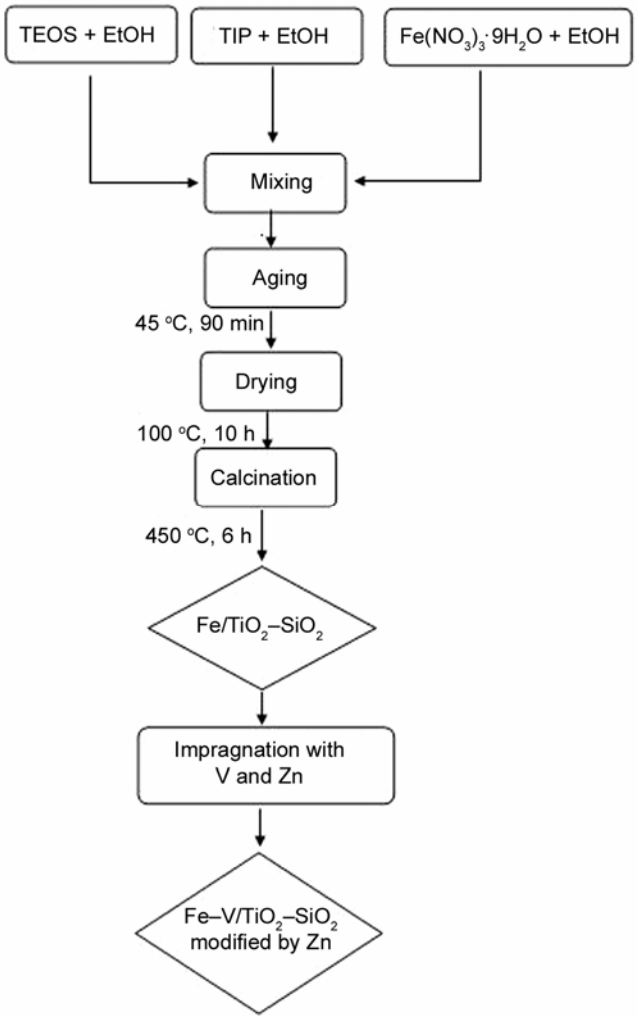

Figure 1. Diagram of the chemical processes for the preparation of Fe–V/TiO_2–SiO_2 samples promoted with zinc.

Table 1. N_2 adsorption–desorption measurements of samples at different synthesis temperatures and different calcination heating rates.

Synthesis temperature (°C)	Heating rates (°C/min)	Specific surface area ($m^2\ g^{-1}$)	Pore diameter (Å)	Ore volume ($cm^3\ g^{-1}$)
25		213·4	0·6864	19·43
35		221·6	0·6895	19·52
45		232·0	0·6973	19·86
55		212·7	0·6714	19·20
65		199·4	0·6608	18·91
75		197·3	0·6563	18·75
	2	189·1	0·5982	18·6
	3	184·2	0·5431	17·98
	4	167·8	0·9380	17·25

getting the best temperature for synthesis, the N_2 absorption–desorption isotherms of samples were taken at different synthesis temperatures to evaluating the specific surface area, pore volume and pore size diameter. The results are depicted in table 1. As can be seen, the synthesis temperature can affect the aforementioned properties of catalyst. Also, it is clear that 45 °C is the best temperature for synthesis of solid magnetic composite sample. The results show that the specific surface area increases with increase in the synthesis temperature. This could imply that enhancing the synthesis temperature increases the dispersion of Fe on TiO_2–SiO_2, which might be a reason for increasing surface characters.

3.2 *Effect of weight ratio of titania to silica*

It is apparent that weight ratio of titania to silica significantly influences on the surface area, pore volume and pore size distribution. N_2 absorption–desorption isotherms of samples were taken for evaluating these effects. Figure 2 represents these characters for catalysts that were prepared with different weight ratios of titania to silica. The obtained results confirmed that the weight ratio can be affected on the surface factors of all the catalysts and showed that equal weight ratio of titania to silica have highest surface area, pore volume and pore diameter and is the best ratio for the catalyst preparation.

3.3 *Effect of Fe loading*

Fe loading is effective on porosity and surface area of nanocatalyst. To indicate this, the N_2 absorption–desorption isotherms of samples were taken for determining the specific surface area. Figure 3 represents these characters for samples which are prepared with different wt% of Fe, it is apparent that amount of Fe significantly influences the surface area, pore volume and pore size distribution of samples. It is probably because of the increasing amount of SiO_2 and TiO_2, which facilitates the high dispersion of the catalyst crystallites. Results show that the specific surface area value for the sample containing 40 wt% of Fe is the highest.

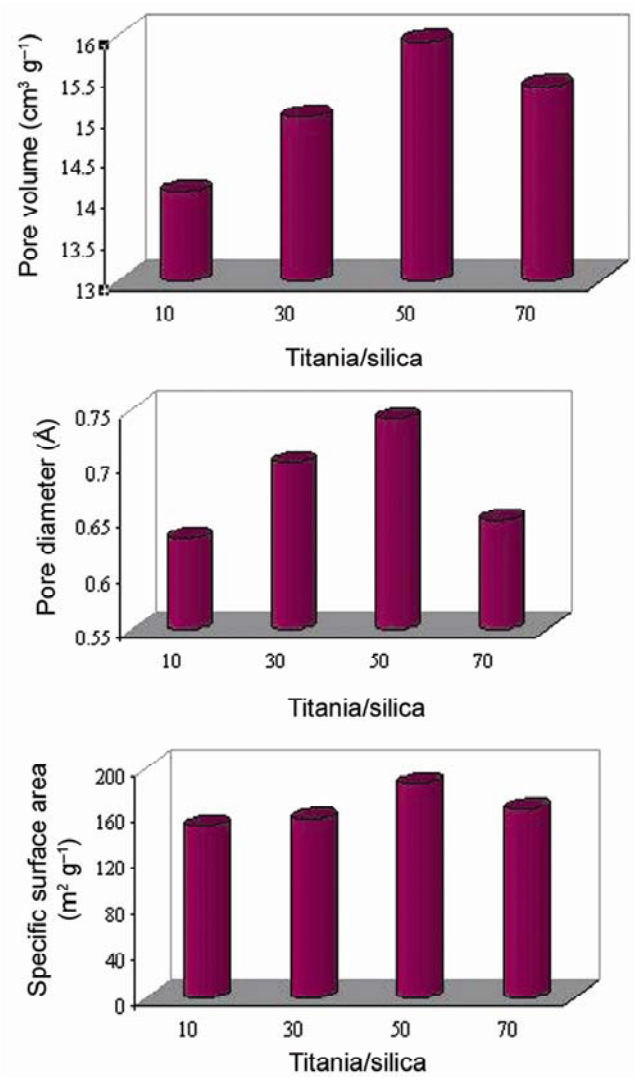

Figure 2. N_2 adsorption–desorption measurements of samples at different weight ratios of titania to silica.

3.4 *Effect of heating rate in calcinations*

For doing this, a series of catalyst precursors that prepared with mentioned optimum conditions were calcined at

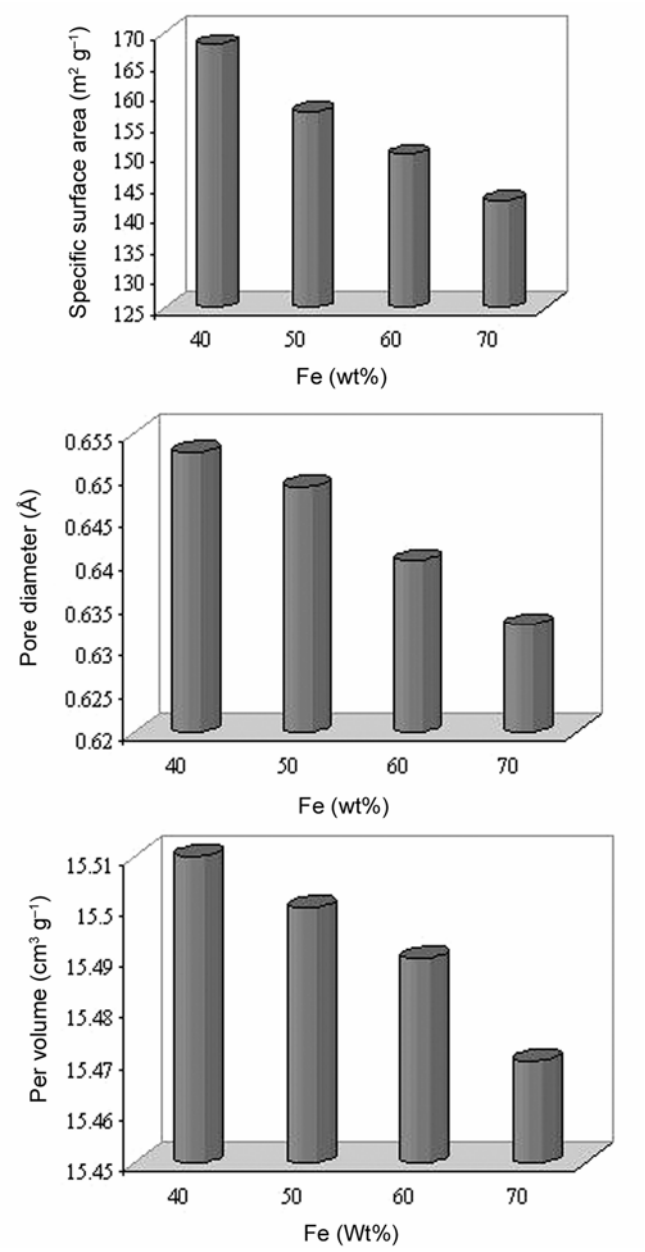

Figure 3. Specific surface area, pore diameter and pore volume of samples at different weight ratios of Fe.

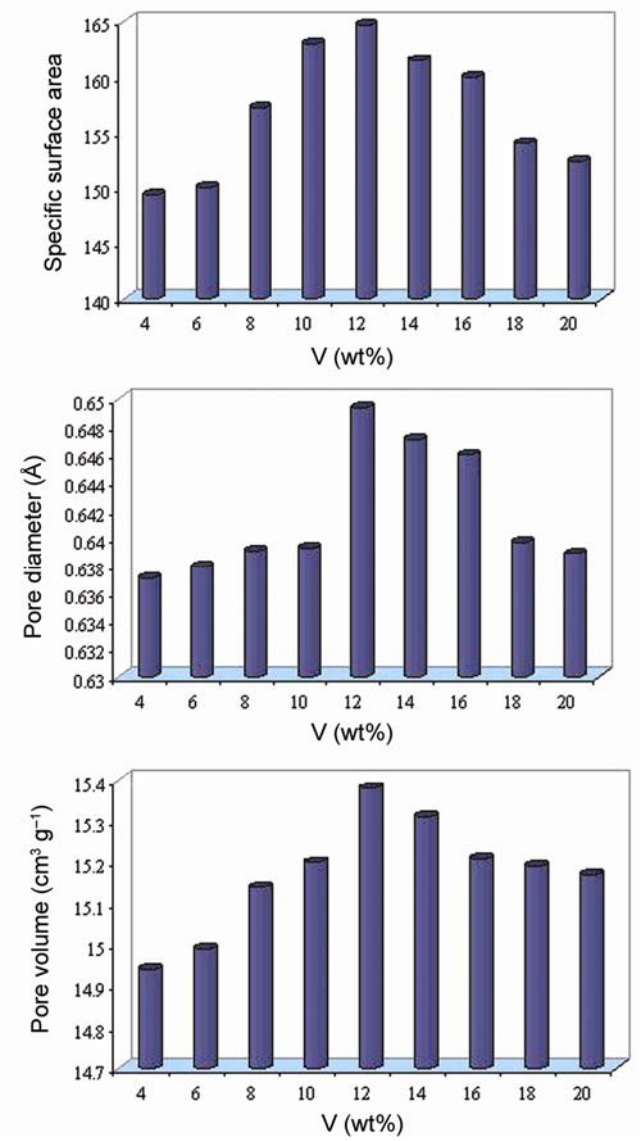

Figure 4. Specific surface area, pore diameter and pore volume of samples at different weight ratios of vanadium.

various heating rates in air. The specific surface areas, pore volumes and pore diameters of the calcined catalysts are given in table 1. Results show that these quantities decrease when heating rate increases from 2 to 4 °C/min. This may be due to the fact that a great deal of heat cannot be emitted within a short period of time, which induces the agglomeration of nanoparticles (Yao *et al* 2005).

3.5 *Effect of vanadium loading*

Figure 4 represents also the results for samples, which are prepared with different weight percentages of V. The results show that vanadium loading can affect the surface characters of catalyst. As can be seen, amount of vanadium, at first, significantly leads to increasing these properties and then they are decreased. Results show that the sample containing 12 wt% of V has highest specific surface area. Decreasing the specific surface area after this value of vanadium may be due to the blockage of the micropores of SiO_2 and TiO_2. This occurs because the impregnation of the support with metal, clogs the pores of the support (Lee and Chen 1997; Therdthianwong *et al* 2008).

3.6 *Effect of zinc loading*

The surface areas and pore size distributions of the Fe–V/TiO_2–SiO_2 samples containing 40 wt% Fe and 12 wt% V

Table 2. N_2 adsorption–desorption measurements of samples for surface properties at different zinc weight percentages.

Zn (wt%)	Specific surface area ($m^2\ g^{-1}$)	Pore diameter (Å)	Pore volume ($cm^3\ g^{-1}$)
0	178·58	0·7278	15·37
2	187·2	0·7426	15·93
4	163·8	0·7134	15·16
6	159·24	0·7011	15·02

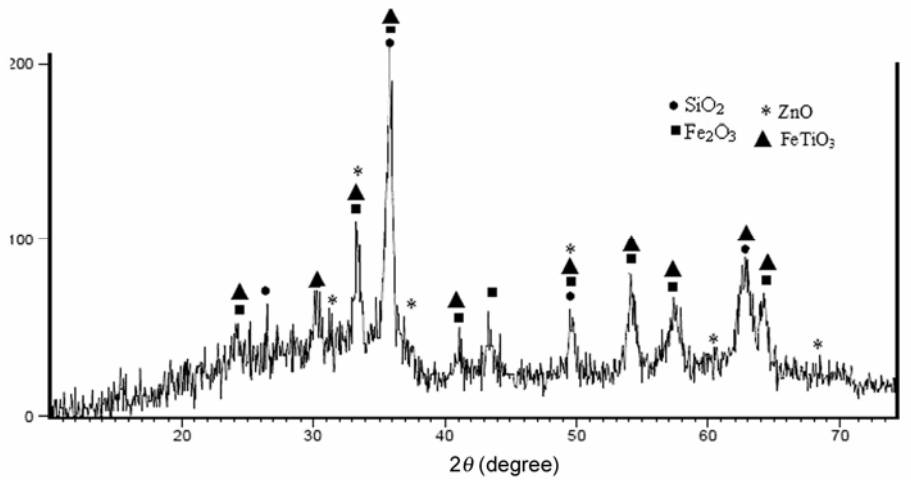

Figure 5. XRD pattern of Fe–V/TiO_2–SiO_2 sample modified by zinc.

that were promoted by different weight percentages of Zn are shown in table 2. It is apparent that zinc promoters significantly influence the surface properties. It can clearly be seen that the addition of small amounts of zinc, increases the surface area of the catalysts, but further increase of it, results in a decrease in surface area. This may be attributed to the improved dispersion of iron and vanadium oxides at low Zn loading (Yu *et al* 2008). As can be seen, after loading of more than 2 wt% of Zn, the gradual decrease in pore volume, pore size and surface area of the catalysts occurred. This decrease in surface area for the sample was noted due to penetration of the active component into the pores of the support. So the optimum value of zinc percent was found to be equal to 2.

Characterization of catalyst with optimum conditions was carried out using various techniques such as XRD, FT-IR, SEM and VSM methods. Figure 5 shows the XRD pattern of the Fe–V/TiO_2–SiO_2 sample modified by zinc containing 40 wt% Fe, 12 wt% V and 2 wt% of Zn. The actual identified phases for this catalyst were Fe_2O_3 (rhombohedral) and SiO_2 (tetragonal). In the XRD pattern of the nanocatalysts, no peak sequence that can be attributed to titanium oxides could be found. It suggested that the addition of Fe^{3+} could occupy regular lattice sites of TiO_2 and might distort crystal structure of the host compound. In addition, no characteristic peaks of vanadium oxide phases were appeared. This implies that vanadium distribution was possibly continuous in the particles (Vejux and Courtine 1978). From the XRD data, the crystallite size (D_c) of the nanocatalysts particles was calculated to be 56 nm, using the Debye–Scherrer equation (Klug and Alexander 1974).

$$D_c = \frac{K\lambda}{\beta \cos\theta}, \tag{1}$$

where β is the breadth of the observed diffraction line at its half intensity maximum, K the so-called shape factor, which usually takes a value of about 0·9 and λ the wavelength of the X-ray source used in the XRD (1·542 Å).

Figure 6 represents the results of SEM recorded in order to demonstrate the morphology and particle size of the catalyst. The SEM images of both precursor and calcined sample are shown. The differences are clear, the image of precursor depicts several larger agglomerations of particles (figure 6a) and shows that this material has a less dense and homogeneous morphology. After the calcination at 450 °C for 6 h, the morphological features show the reduction of the agglomerate size (figure 6b). It may be assigned to the covering of calcined sample surface by small crystallite of iron oxides. The average particle size of this nanocatalyst obtained was 61 nm, which is in agreement with XRD result (56 nm).

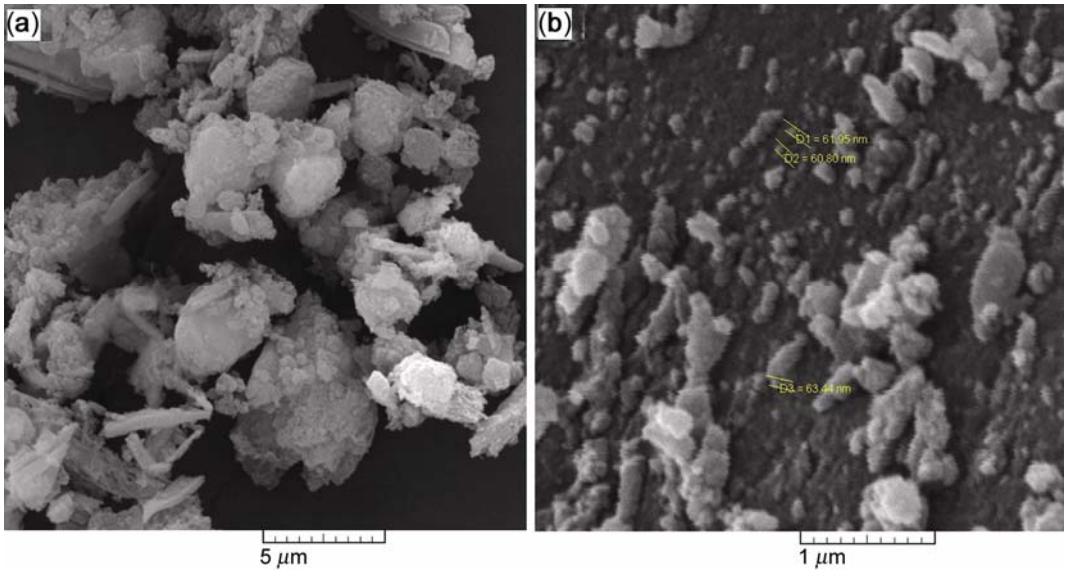

Figure 6. SEM images of Fe–V/TiO_2–SiO_2 sample modified by Zn: (**a**) precursor and (**b**) calcined sample.

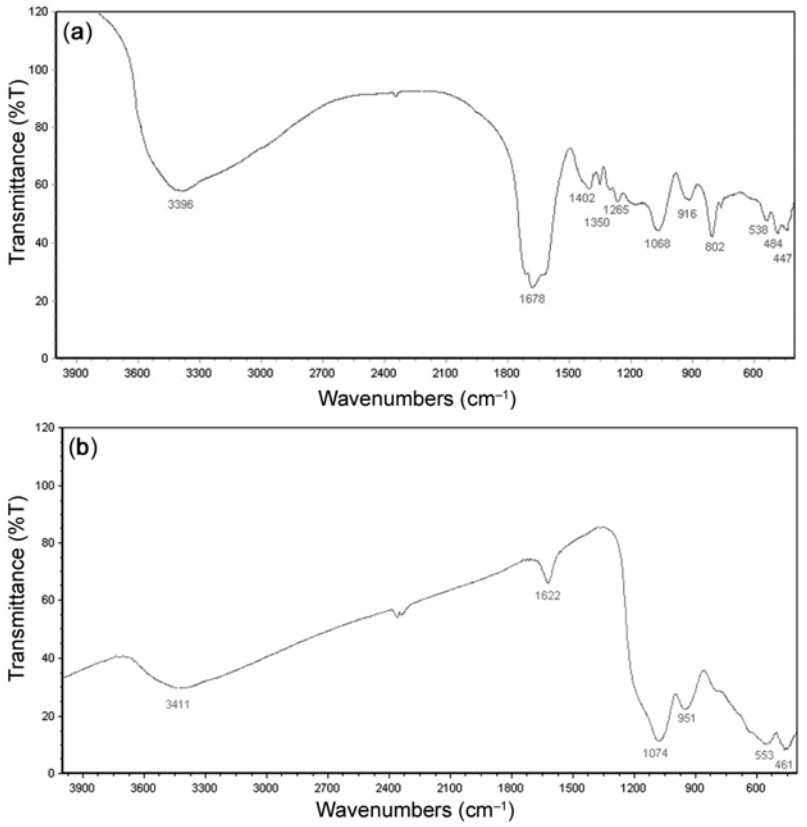

Figure 7. FT-IR spectra of the Fe–V/TiO_2–SiO_2 promoted with zinc: (**a**) precursor and (**b**) calcined sample.

The magnetization measurement for the prepared nanocatalyst was carried out using a VSM at room temperature with an applied magnetic field of ± 10,000 kOe. The observed value of saturation magnetization of the sample was 10·23 emu/g.

FT-IR spectroscopy is used to get detailed information about the surface structure through the modes of vibration and results are displayed in figure 7. The bands at 1068 and 484 cm^{-1} correspond to asymmetric stretching and bending modes of Si–O–Si linkage in precursor and those

at 461 and 1074 cm^{-1} attributed to the calcined catalyst (El Shafei and Mokhtar 1995; Mohamed *et al* 2002). The Ti–O–Si infrared vibration is generally observed between 910 and 960 cm^{-1} (Kochkar and Figueras 1997; Gao and Wachs 1999) with the exact band position depending on the chemical composition of the sample as well as calibration and resolution of the instrument. In the spectrum of pure TiO_2, the peak at 550 cm^{-1} shows stretching vibrations of Ti–O and peak at 1450 cm^{-1} shows stretching vibrations of Ti–O–Ti. The spectrum of TiO_2–SiO_2 shows the peaks at 1400 cm^{1} and about 450–550 cm^{-1} exhibiting stretching modes of Ti–O–Ti (Balachandaran *et al* 2010). The band around 2300 cm^{-1} corresponds to Fe–O–Ti in both the precursor and calcined samples (Luu *et al* 2010). The bands at 538 and 553 cm^{-1} can be assigned to the Fe–O stretching in Fe–O–Si bonds in precursor and calcined catalyst, respectively. These results suggested that the Fe–SiO_2 interaction exists in the catalyst in the form of Fe–O–Si structure (Predoi *et al* 2007).

3.7 *Catalytic performance*

The synthesized optimal nanocatalysts (Fe–V/TiO_2–SiO_2 containing 40% Fe, 12% V that was promoted with 2 wt% of Zn) were employed for oxidation reaction of alcohols to aldehydes and ketones. We carry out these reactions under atmospheric oxygen (scheme 1).

The progress of reactions was monitored by TLC. Table 3 gives the oxidation results. Compared to what Velusamy and Punniyamurthy (2004) reported, our catalyst has a better performance for mentioned reactions. The observed shorter reaction times compared to their catalyst can be interpreted by considering the fact that Fe–V/TiO_2–SiO_2 nanocatalyst has a higher surface area. Also, after completion of the reactions, recovery of Fe–V/TiO_2–SiO_2 nanocatalyst from the reaction mixtures was easily achieved by applying an external permanent magnet on the outside wall of the reaction tubes, as shown in figure 8. Therefore, the products were isolated in good purity after the volatile portions were removed and the product was purified. All isolated products gave satisfactory spectral data (^{1}H NMR) compared with those reported in literature (Velusamy and Punniyamurthy 2004). At the end of the reaction, to determine the applicability of catalyst recovery, we decanted the vessel by use of an external magnet and remaining catalyst was

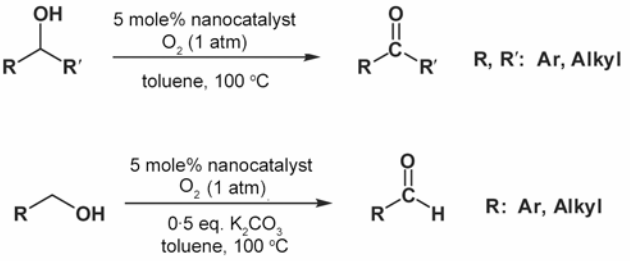

Scheme 1. Fe–V/TiO_2–SiO_2 catalyzed oxidation reactions.

Table 3. Catalyzed oxidation reactions.

Entry	Substrate	Product	Time (h)	M.P. (°C) found	M.P. (°C) reported (Backingham and Macdonald 1996)	Yield
1	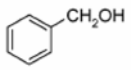	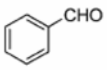	14	Oil	–26	92
2	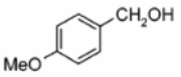	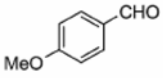	18	Oil	0	95
3	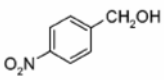	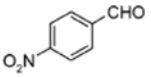	21	104	105	93
4	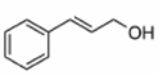	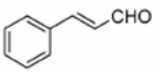	12·5	Oil	–7·5	93
5			8·5	19	20	91
6	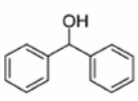	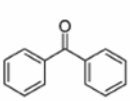	14	48	48	90

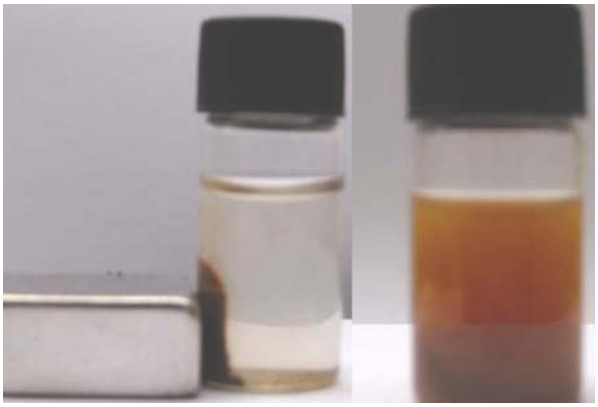

Figure 8. Recovery of catalyst (left) from medium (right) by a magnet.

washed with diethyl ether to remove residual product and it then dried under vacuum. The recovered nanocatalyst was reused for the subsequent reaction. Results show that the catalytic activity and recovery rate of this magnetic composite catalyst can be well maintained after four cycles of catalysis.

4. Conclusions

Fe–V/TiO_2–SiO_2 nanocatalysts modified by zinc were prepared and characterized. The structure, morphology, porosity, surface area and particle size of this catalyst were found to be dependent on the methods and preparation conditions. Results revealed that Fe–V/TiO_2–SiO_2 sample modified by zinc containing 40 wt% of Fe and 12 wt% of V, which was promoted by 2 wt% of zinc and equal mole ratio of titania to silica, has the highest values of specific surface area, pore volume and pore diameter. The optimum temperature for synthesis was found to be equal to 45 °C. The XRD pattern for nanocatalyst showed that Fe_2O_3 phase is present at rhombohedral form while the SiO_2 phase is present at tetragonal system. Debye–Scherrer equation was shown that nanocatalyst has a particle size about 56 nm in accordance with SEM results (61 nm) and the M_s factor (saturation magnetization) of nanocatalyst which was determined by VSM technique was equal to 10·173 emu/g. The catalyst can easily be separated from medium by a magnet.

References

Arakawa H and Bell A T 1983 *Ind. Eng. Chem. Process. Des. Dev.* **22** 97

Backingham J and Macdonald F 1996 Dictionary of organic compounds (London: Chapman and Hall)

Balachandaran K, Venckatesh R and Rajeshwari S 2010 *Int. J. Eng. Sci. Technol.* **2** 3695

El Shafei G M and Mokhtar M M 1995 *Colloid. Surf.* **A94** 267

Gao X T, Bare S R, Fierro J L G and Wachs I E 1999 *J. Phys. Chem.* **B103** 618

Gao X and Wachs I E 1999 *Catal. Today* **51** 233

Goehre O and Friedrichsen W 1969 UK Patent GB1140264

Gutiérrez-Alejandre A, González-Cruz M, Trombetta M, Busca G and Ramírez J 1998 *Microp. Mesop. Mater.* **23** 265

Handy B E, Baiker A, Schraml-Marth M and Wokaun A 1992 *J. Catal.* **133** 1

Hu H and Waches I E 1995 *J. Phys. Chem.* **99** 10911

Klug H P and Alexander L E 1974 X-ray diffraction procedures for polycrystalline and amorphous materials (New York: Wiley) 2nd edn

Kobayashi M K, Kuma R, Masaki S and Sugishima N 2005 *Appl. Catal.* **B60** 173

Kochkar H and Figueras F 1997 *J. Catal.* **171** 420

Lakshmi L J, Alyea E C, Srinivas S T and Rao P K 1997 *J. Phys. Chem.* **B101** 33243

Lee C H and Chen Y W 1997 *Ind. Eng. Chem. Res.* **36** 1498

Li S, Krisyhnamoorthy S, Li A, Meitzner G D and Iglesia E 2002 *J. Catal.* **206** 202

Luu C L, Nguyen Q T and Ho S T 2010 *Adv. Nat. Sci. Nanosci. Nanotechnol.* **1** 5

Mohamed M M, Salama T M and Yamaguchi T 2002 *Colloid. Surf.* **A207** 25

Predoi D, Crisan O, Jitianu A, Valsangiacom M C, Raileanu M, Crisan M and Zaharescu M 2007 *Thin Solid Films* **51** 6319

Rana M S, Maity S K, Ancheyta J, Murli Dhar G and Prasada T S R 2003 *Appl. Catal.* **A253** 165

Samantaray S K and Parida K M 2001 *Appl. Catal.* **A211** 175

Tsang S C, Caps V, Paraskevas I, Chadwick D and Thompsett D 2004 *Angew. Chem. Int. Ed.* **43** 5645

Therdthianwong S, Siangchin C and Therdthianwong 2008 *Fuel Process. Technol.* **89** 160

Van Hengstum A J, Ommen Van J G, Bosch H and Gellings P J 1983 *Appl. Catal.* **8** 369

Velusamy S and Punniyamurthy T 2004 *Org. Lett.* **6** 217

Vejux A and Courtine P 1978 *J. Solid State Chem.* **23** 93

Yang Y, Xiang H W, Xu Y Y, Bai L and Li Y W 2004 *Appl. Catal.* **A266** 181

Yao X, Dong W, Yuhan S, Zhijie L and Bo H J 2005 *Mater. Sci.* **40** 3939

Yu W, Wu B, Xu J, Tao Z, Xiang H and Li Y 2008 *Catal. Lett.* **125** 116

Zhang C, Teng B, Yang Y, Tao Z, Hao Q, Wan H, Yi F, Xu B, Xiang H and Li Y 2005 *J. Mol. Catal.* **A239** 15

Zhang C H, Yang Y, Teng B T, Li T Z, Zheng H Y, Xiang H W and Li Y W 2006 *J. Catal.* **237** 405